Simulation of Amplitude Behaviour in the Ag^+ Perturbed Excitable Belousov-Zhabotinsky Reaction by the Oregonator Model

Peter Ruoff
Department of Chemistry, University of Oslo, Norway

Z. Naturforsch. **38 a**, 974–979 (1983); received April 18, 1983

Potentiometric measurements with platinum and silver electrodes of Ag^+ induced oscillations in the oxygen-inhibited excitable Belousov-Zhabotinsky system are reported. Calculations based on the Oregonator model lead to the conclusion that the platinum electrode's potential is composed of two contributions, the Ce(III)/Ce(IV) redox couple which dominates at low Ag^+ flow rates and the contribution of $HBrO_2$, HOBr and BrO_2 which dominates at higher Ag^+ addition rates.

Introduction

Among the various chemical reactions involving oscillations, the Belousov-Zhabotinsky reaction (BZR) [1–3] is very remarkable. It is defined as a metal-ion catalyzed oxidation of easily brominated organic material by bromate ions in aqueous acidic media [4]. Field, Körös and Noyes have suggested a mechanism [3] which explains most of the observed phenomena. In this mechanism, Br^- ions play the role of a switching parameter, turning the autocatalytic production of $HBrO_2$ on and off. On the basis of the FKN mechanism several mathematical models have been constructed [5–9]. One of the first and most thoroughly investigated is the so-called Oregonator model [5], which often serves as a basis for more sophisticated simulation models. Although it is only a three-variable model, it describes semi-quantitatively most of the experimental observations.

However, recently Noszticzius [10] reported "non-bromide controlled" oscillations, i.e. he still observed oscillations at the platinum electrode (PE) when $AgNO_3$ is added in excess such that the Br^- concentration is driven far below the previous Br^- concentration value which is expected to control the oscillations. This and other [11–13] observations led Noszticzius and Farkas [14] and Noszticzius and Feller [15] to look for a "bromide-free" model of the BZR. Ganapathisubramanian and Noyes [16] confirmed and somewhat extended Noszticzius' results and postulated an alternative method of control by bromine atoms.

Reprint requests to P. Ruoff, Department of Chemistry, University of Oslo, P. O. B. 1033, Blindern, Oslo 3, Norway.

Recently, we reported of $AgNO_3$ induced oscillations in the quiescent excitable BZR [17]. These oscillations show a close relationship and analogous behaviour to Noszticzius' observations, i.e. we also observe an increase in frequency and a drastic decrease in the amplitude of the Br^- detecting electrode. We deduced a simple semi-quantitative relationship between added $AgNO_3$ and observed frequency [18].

In this paper we show that in the excitable BZR the Oregonator model is able to describe the amplitudes of the Br^- detecting silver electrode (SE) and the PE semi-quantitatively. However, the assumption has to be made, that the PE is not only able to detect Ce(IV) but also intermediates which are dynamically closely connected to $HBrO_2$. Based on this assumption, we further show that experimental phase plots, in a first approximation, may be regarded as a rotation of the three-dimensional Oregonator limit cycle mapped onto the concentration plane spanned by the PE and SE.

Experimental Section and Method of Calculation

Addition of $AgNO_3$ into the excitable BZR was performed as described in a previous paper [18]. Amplitudes were measured using the mean of the first 5–10 SE cycles and the corresponding PE oscillations. In all experiments the following initial reagent concentrations were used: 1 M H_2SO_4, 0.28 M malonic acid, $2.1 \cdot 10^{-3}$ M $(NH_4)_2Ce(NO_3)_6$ and 0.1 M $KBrO_3$. The reactants were always mixed in the order H_2SO_4 – malonic acid – Ce(IV) – and finally $KBrO_3$. In the "normal" oscillating BZR experimental phase plots were recorded by using a

0340-4811 / 83 / 0900-0974 $ 01.3 0/0. – Please order a reprint rather than making your own copy.

$X-Y$ plotter. The temperature was kept constant at 25 °C.

Simulation calculations were performed on a CDC CYBER 170 computer using the program package DARE P with a version of Gear's algorithm [19]. An extended Oregonator model with a fast Br^- removing reaction was used ($Y=Br^-$)

$$Y + Ag^+ \xrightarrow{k_6} AgY^+. \quad (1)$$

Except for the parameter $k'_6 = [Ag^+] \cdot k_6$ and f, all parameters were taken from ref. 5. The model is treated as an open system with respect to Ag^+, i.e. with k'_6 as a time constant. Before solving the differential equations numerically, they were cast into the dimensionless variables α, η and τ. Amplitudes of the logarithms of X, Y and Z ($X=HBrO_2$, $Z=Ce(IV)$) were determined with f and k'_6 as variable parameters. In the numerical results reported here f was kept constant at 4.0.

Results and Discussion

When $AgNO_3$ is added to an excitable BZR, we observe an increase in frequency [18] and a rapid fall of the amplitude of the Br^- detecting SE, whereas the amplitude of the PE, in comparison, hardly changes. Finally, at high addition rates of $AgNO_3$ or sufficiently increased $AgNO_3$ concentrations we observe a nonoscillatory response.

As indicated by a simple qualitative "back-on-the-envelope-calculation" [18] this behaviour may be understood since in stages of the cycle where the Br^- concentration is high ($c_{Br^-} > c_{crit}$ and Ce(IV) reacts with organic material) the Ag^+ addition results, due to the formation of AgBr, in a decrease of the Br^- concentration. Therefore the period length *and* the Ce(IV) and Br^- amplitudes should decrease. On the other hand, when the Br^- concentration is already low ($c_{Br^-} < c_{crit}$ and, in addition, Ce(III) is oxidized to Ce(IV)) the addition of Ag^+ should practically have no influence (except for very high Ag^+ addition rates). This is exactly the behaviour which is found in the Oregonator model.

Figure 1 A shows the amplitude change of the PE and SE as a function of addition rate, using a 0.05 M $AgNO_3$ solution. The relationship between PE and SE amplitudes is given in Figure 1 B. Figure 2 shows the behaviour of small amplitude oscillations observed at the border between oscillatory and quiescent domain.

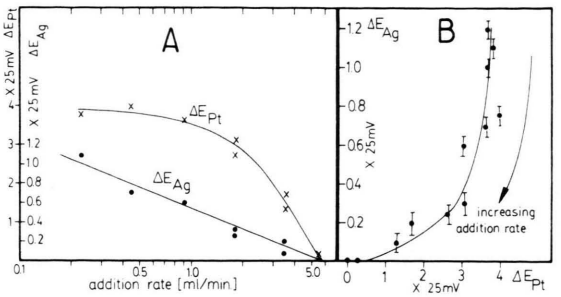

Fig. 1. Experimental amplitude behaviour of oscillations induced by pumping a 0.05 M $AgNO_3$ solution into the excitable BZR. Vertical bars indicate uncertainty in measured SE amplitudes.

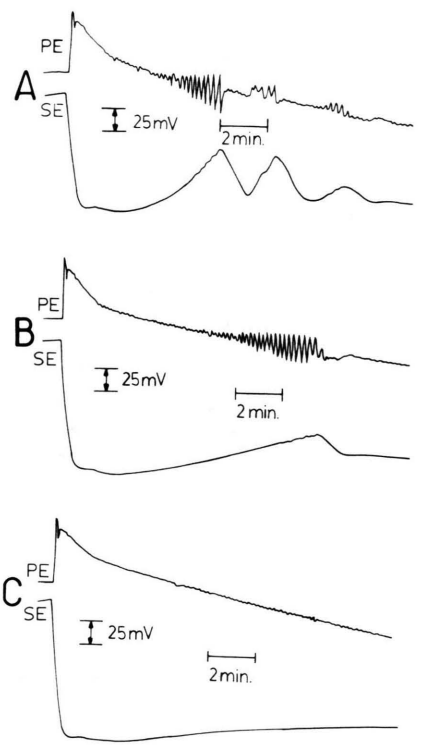

Fig. 2. Transition from $AgNO_3$ induced oscillating regime to quiescent domain by slight increase of $AgNO_3$ concentration. A) 0.05 M $AgNO_3$, B) 0.063 M $AgNO_3$, and C) 0.075 M $AgNO_3$. Addition rate: 3.62 ml/min.

In previous papers [17, 18] we assumed that the potentials of the PE and SE reflect qualitatively the change of $\log(Ce^{4+}/Ce^{3+})$ and $\log(Br^-)$ respectively. However, experimental investigations [20–25] indicate that the PE's potential may be the result of several contributing species especially Ce(IV), HOBr and BrO_2.

Table 1. $\log(X_{max}/X_{min})$ and $\log(Z_{max}/Z_{min})$ as a function of k_6'.

k_6'	$\log(X_{max}/X_{min})$	$\log(Z_{max}/Z_{min})$
100	4.99	1.45
400	4.94	0.90
800	4.86	0.63
1200	4.77	0.49
2000	4.62	0.33
4000	3.91	0.16
5000	3.05	0.12

In fact, making that assumption, we are able to interpret several unexplained observations.

As indicated by the model of Edelson et al. [6], the intermediates in the two groups ($HBrO_2$, HOBr, BrO_2) and (Ce(IV), Br_2) seem to behave quite similarly. Thus X and Z of the Oregonator model, in a first approximation, may also stand for these intermediates. In the present paper we will use this interpretation of X and Z.

Because the X and Z pulse occur almost simultaneously in the Oregonator model, the higher Z concentration and the broader Z pulse may under normal oscillating conditions dominate and partially or completely cover the tiny X pulse, such that the PE's potential mainly shows the Z variation [21, 22]. On the other hand, adding the fast Br^- removing term to the Oregonator, the X and Z amplitudes begin to differ quite markedly, i.e. the Z amplitude is rapidly decreasing under increased Br^- removal, while the X amplitude decreases much slower (Table 1). Thus, if the Oregonator gives a qualitative correct description of the situation, the PE should become more and more sensitive to X, since the Z contribution to the PE's potential becomes an additive "background constant". At higher $AgNO_3$ addition rates it therefore appears reasonable that the PE's potential shows a superposition of the X and Z contributions. This is indicated in Figure 3A. However, the superposition should change by varying the $AgNO_3$ addition rate, since a variation of the Z pulse (Table 1) should change its contribution to the spike. In this respect we have analyzed the form of PE potentials at several addition rates and $AgNO_3$ concentrations and found a qualitative agreement with experiment (Fig. 3 and Table 2).

As a consequence, the X amplitudes in the Oregonator should qualitatively correlate to the experimental PE amplitudes. This is indeed the case

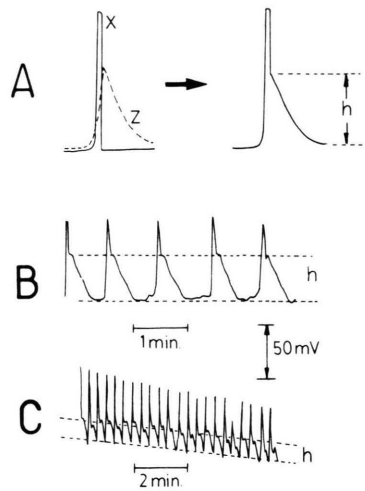

Fig. 3. A) Superposition of X and Z contributions to PE's potential under $AgNO_3$ addition; B) Experimental record of PE potential. Addition rate: 0.92 ml/min, $AgNO_3$ concentration: 0.05 M; C) Experimental record of PE potential. Addition rate: 1.82 ml/min, $AgNO_3$ concentration: 0.1 M. In agreement with calculations (Table 1) a decrease of the Z contribution h is observed under increased $AgNO_3$ addition.

Table 2. h as a function of $AgNO_3$ addition.

h (% of entire pulse)	Addition rate[a]	Concentration of $AgNO_3$[b]
55	0.92	0.05
53	0.92	0.1
47	1.82	0.05
33	3.62	0.05
24	1.82	0.1

[a] in ml/min. [b] in mole/dm^3.

as shown in Figure 4. Figure 4A shows how the X amplitude changes with increasing k_6', whereas Fig. 4B gives the relation between X and Y amplitudes. Compared with Fig. 1, we get a semi-quantitative agreement with experiment.

Further, the sensitivity of the PE to both X and Z may not only account for the observed shape of the PE pulse (Fig. 3) but has also interesting consequences on phase plots. If it is assumed that the PE is mainly sensitive to Ce(IV) and the SE mainly to Br^-, one should observe a phase plot qualitatively similar to the Oregonator portrait (Fig. 3, Ref. [5]). Instead, we observe a self-intersecting curve as shown in Figure 5A. However, this form is qualitatively obtained, if we assume an additional sen-

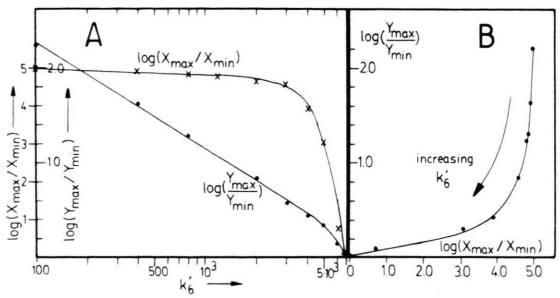

Fig. 4. Amplitude behaviour in the excitable Oregonator ($f = 4.0$) with a fast Br^- removing reaction ($k_6' = k_6[AgNO_3]$).

sitivity of the electrodes to X and Z-like intermediates.

The sensitivity of an electrode to an additional perturbing species may *approximately* be regarded as the result of rotated and projected concentration axes onto the electrode's potential axis as indicated in Fig. 6 in the appendix. There it is shown, that for small rotation angles (which may be regarded as a measure of the electrode's sensitivity to the perturbing species) this geometrical interpretation leads to an expression analogous to the Nikolsky equation [26], which, in a first approximation, describes the influence of a perturbing species on the measured potential. Thus, the sensitivity of an electrode to another intermediate in the BZR has the effect that we observe a *rotated* limit cycle projected onto the electrode axes. Indeed, in "simulation experiments" where the horizontal and vertical axes of the computer plotter are regarded as the analog to the experimental electrode axes PE and SE, we found rotations such that experimental phase plots and projected limit cycle are in qualitative agreement (Figure 5). Although the projected limit cycle does not have the smooth appearance of the experimental phase plot, the main characteristics fit well, i.e. correct time evolution, and the slow and fast parts in the experimental plot correlates with the corresponding parts in the projected limit cycle.

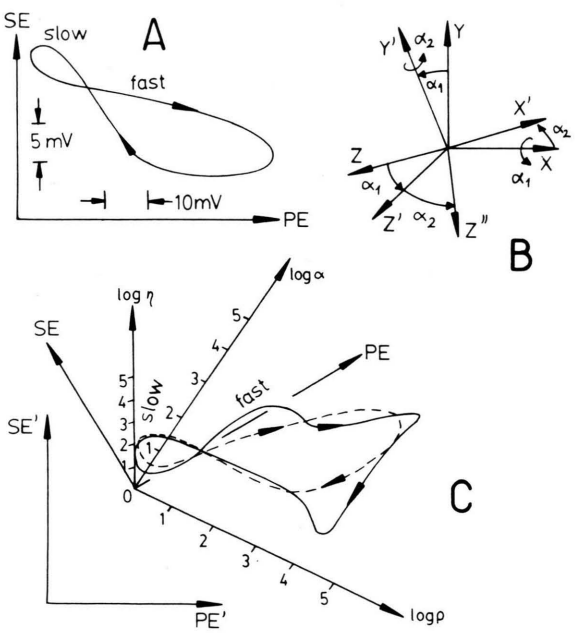

Fig. 5. A) Experimental phase plot of BZR under "normal" oscillating conditions. B) Rotating the Oregonator limit cycle in concentration space. To start with, the X ($\log \alpha$) and Y ($\log \eta$) axes lie in the paper plane with Z ($\log \varrho$) orthogonal to them. Then rotations around the X axis ($\alpha_1 = 60°$) and Y axis ($\alpha_2 = 55°$) are performed. C) Effect of rotations described in B and final projection of Oregonator cycle onto the plotter axes PE′ and SE′. The dashed curve is the experimental phase plot.

The Oregonator gives semi-quantitative agreement with our experiments, but apparently does not give any information about the factors which might control the oscillations at low Br^- concentrations. But the fact that the Oregonator shows the correct trend under various addition rates, it appears, however, that the control is already inherent in the FKN mechanism. In fact, taking the Oregonator literally, it predicts such a control already by the disproportionation reaction of $HBrO_2$! Ganapathisubramanian and Noyes [16] have studied several ways of $HBrO_2$ control at low Br^- concentrations, although they did not consider a $HBrO_2$ self-controlled system.

In the limit, when the SE potential tends to zero, we observe more or less marked bursts (Fig. 2 and Fig. 1 B in [19]). As shown by Janz et al. [8] and by Rinzel and Troy [9], bursts may occur because the system is close to the border between an oscillatory and quiescent (steady) state and sweeps between these two domains. It seems that this is what happens with our system, since we are very close to such a border. In addition, it is interesting to note, that the behaviour of f in the model is quite analogous to the SE's response in the bursting domain (Fig. 2; and Fig. 5 in [8]).

It seems reasonable to make the same or similar assumptions upon the PE also for Ag^+ perturbed *oscillating* BZRs. Until now, only qualitative data on change in amplitude and frequency have been

reported. However, the results by Noszticzius [10] and by Ganapathisubramanian and Noyes [16] indicate that similar relationships may hold as in the excitable BZR. We have varied f in our extended Oregonator model in the range $1 \leqq f \leqq 8$ and found the same types of curves as in Figure 4. Thus, the Oregonator or similar models may probably also be applied to the Ag^+ perturbed oscillatory BZR. However, when the SE amplitude tends to zero, the Oregonator predicts a zero PE amplitude, while experiments still show small amplitude oscillations at the PE [10, 16]. This effect still awaits a thorough explanation, although it is our impression that it is caused by secondary electrode processes at the Br^--selective electrode. In solutions where the Br^- concentration is buffered below 10^{-7} M, Ganapathisubramanian and Noyes [27] observed increased response times of the Br^--selective electrode of about 1 min. On the other hand, the oscillation period in $AgNO_3$ perturbed BZRs is generally shorter than under normal oscillating conditions [10] and may even shrink to about 15 s [18]. These two opposite trends (increased response time and decrease in period) may eventually create a situation where the response time of the Br^--selective electrode is too high to follow the oscillations.

The Oregonator is only a skeleton of the entire FKN mechanism, and although it reproduces the main trends in frequency [18] and amplitude over a considerable range of $AgNO_3$ addition rates, the details still remain uncertain. However, we think that the viewpoint of the electrodes' role in the BZR presented above may be useful in order to understand the amplitude behaviour in $AgNO_3$ perturbed excitable BZRs within the frame of the FKN mechanism.

Further calculations on more realistic models with complementary experiments are considered.

Appendix

In the presence of a perturbing species S, the potential measurement of species M is in a first order approximation described by the following equation [26]

$$\Delta\Phi = \Delta\Phi' \pm (RT/Z_M F) \cdot \log[a_M + K_{MS}(a_S)^{Z_M/Z_S}]^* . \quad (2)$$

* here $\log \equiv \log_e$.

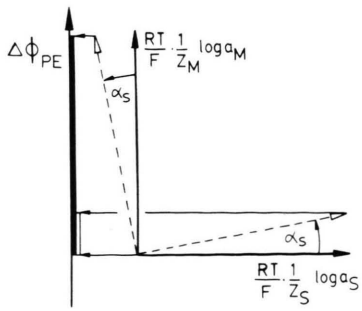

Fig. 6. Geometrical interpretation of a perturbing species' effect upon the PE's potential $\Delta\Phi_{PE}$. In ideal unperturbed potential measurements of M, the potential axis $\Delta\Phi_{PE}$ and the concentration axis $\log(a_M)$ are parallel. The measurement is interpreted as a projection of $\log(a_M)$ onto $\Delta\Phi_{PE}$. A perturbing species S is introduced by rotating the (to $\log(a_M)$ orthogonal) $\log(a_S)$ axis in direction to $\Delta\Phi_{PE}$. The resulting observed potential is the projection of the concentration axes onto $\Delta\Phi_{PE}$.

The Φ's denote the potentials and R, T, and F the gas constant, the absolute temperature, and the Faraday constant respectively. K_{MS} is the selectivity constant and Z_M or Z_S is the charge or change in charge of the species M or S. The a_M and a_S denote the activity of M and S.

Let us assume that the PE measures mainly species M, but that its potential ($\Delta\Phi_{PE}$) is perturbed by species S, with its concentration axis orthogonal to the $\log(a_M)$ axis. The perturbation may be regarded as a small rotation (with angle α_S) around an axis orthogonal to both the $\log(a_M)$ and $\log(a_S)$ axes (Figure 6).

We may write:

$$\Delta\Phi_{PE} = (RT/F)\left(\cos(\alpha_s)\left(\frac{1}{Z_M}\right)\log(a_M) + \sin(a_s)\left(\frac{1}{Z_S}\right)\log(a_s)\right) \quad (3)$$

$$= (RT/FZ_M)(\cos(\alpha_S)\log(a_M) + \sin(\alpha_S)\log(a_S)^{Z_M/Z_S}) \quad (4)$$

$$\approx (RT/FZ_M)(\log(a_M) + \alpha_S a_S^{Z_M/Z_S}) + \Delta\Phi', \quad (5)$$

where we used the following expressions:

$$\cos(\alpha_S) \approx 1, \quad \text{and} \quad \sin(\alpha_S) \approx \alpha_S, \quad \alpha_S \text{ small} \quad (6)$$

$$\log(x) \approx x - 1, \quad x \approx 1 \quad (7)$$

and

$$\Delta\Phi' = -\alpha_S (RT/F \cdot Z_M) . \tag{8}$$

Introducing the selectivity constant $K_{MS} = \alpha_S a_M$, we obtain:

$$\Delta\Phi_{PE} = (RT/FZ_M)\left(\log(a_M) + K_{MS}\frac{(a_S)^{Z_M/Z_S}}{a_M}\right) + \Delta\Phi' . \tag{9}$$

Using again the approximative expression (7) we finally get

$$\approx (RT/FZ_M)\left(\log(a_M) + \log\left(1 + K_{MS}\frac{(a_S)^{Z_M/Z_S}}{a_M}\right)\right) + \Delta\Phi' \tag{10}$$

$$= (RT/FZ_M)\log[a_M + K_{MS}(a_S)^{Z_M/Z_S}] + \Delta\Phi' , \tag{11}$$

where (11) is analogous to the Nikolsky equation (2).

[1] B. P. Belousov, Ref. Radiats Med. **1958,** 145 (1959).
[2] A. M. Zhabotinsky, Dokl. Akad. Nauk SSSR, **157,** 392 (1964).
[3] R. J. Field, E. Körös, and R. M. Noyes, J. Amer. Chem. Soc. **94,** 8649 (1972).
[4] R. J. Field, in Theoretical Chemistry, Vol. 4, eds. H. Eyring and D. Henderson, Academic Press, New York 1978.
[5] R. J. Field and R. M. Noyes, J. Chem. Phys. **60,** 1877 (1974).
[6] D. Edelson, R. J. Field, and R. M. Noyes, Int. J. Chem. Kinet. **VII,** 417 (1975).
[7] D. Edelson, R. M. Noyes, and R. J. Field, Int. J. Chem. Kinet. **XI,** 155 (1979).
[8] R. D. Janz, D. J. Vanecek, and R. J. Field, J. Chem. Phys. **73,** 3132 (1980).
[9] J. Rinzel and W. C. Troy, J. Chem. Phys. **76,** 1775 (1982).
[10] Z. Noszticzius, J. Amer. Chem. Soc. **101,** 3660 (1979).
[11] Z. Noszticzius and J. Bódiss, J. Amer. Chem. Soc. **101,** 3177 (1979).
[12] Z. Noszticzius, Magyar Kémiai Folóirat **85,** 330 (1979).
[13] Z. Noszticzius, Acta Chim. Acad. Sci. Hung. **106,** 347 (1981).
[14] Z. Noszticzius and H. Farkas, in Modelling of Chemical Reaction Systems, eds. K. M. Ebert, P. Deuflhard and W. Jäger, Springer-Verlag, Berlin 1981.
[15] Z. Noszticzius and A. Feller, Acta Chim. Acad. Sci. Hung. **110,** 261 (1981).
[16] N. Ganapathisubramanian and R. M. Noyes, J. Phys. Chem. **86,** 5155 (1982).
[17] P. Ruoff, Chem. Phys. Letters **90,** 76 (1982).
[18] P. Ruoff, Chem. Phys. Letters **92,** 239 (1982).
[19] J. V. Wait and D. Clarke, DARE P User's Manual, Version 4, Report 299, University of Arizona 1976.
[20] U. Franck and W. Geiseler, Naturwiss. **58,** 52 (1971).
[21] L. Treindl and V. Dorovský, Z. Phys. Chem. N. F. **126,** 129 (1981).
[22] L. Treindl and V. Dorovský, Collect. Czech. Chem. Commun. **47,** 2831 (1982).
[23] H. D. Försterling, H. Schreiber, and W. Zittlau, Z. Naturforsch. **33a,** 1552 (1978).
[24] H. D. Försterling, H. Lamberz, and H. Schreiber, Z. Naturforsch. **35a,** 329 (1980).
[25] H. D. Försterling, H. J. Lamberz, H. Schreiber, and W. Zittlau, Acta Chim. Acad. Sci. Hung. **110,** 251 (1982).
[26] K. Camman, Das Arbeiten mit ionenselektiven Elektroden, Springer-Verlag, Berlin 1973, Chapter 1.5.
[27] N. Ganapathisubramanian and R. M. Noyes, J. Phys. Chem. **86,** 3217 (1982).